Research Article

Fast statistical energy analysis modelling of periodic box-like structures

Feng Yan[1] · Robin Wilson[2] · Peter Rutherford[2]

Received: 10 December 2021 / Accepted: 24 February 2022
Published online: 28 March 2022

Abstract
This paper proposes a fast way to create a base Statistical Energy Analysis (SEA) model for periodic box-like structures, for which further refining and modification can be conducted with simplicity. A novel numbering system is introduced which enables the model builder to build, locate and change the property of each subsystem as well as to specify the connections between different subsystems in a 3D coordinate system. Two numerical SEA models are studied with the aid of the new method. It greatly decreases the time in model building and increases the simplicity of studying the acoustic attenuation by changing the properties of different subsystems. The results show that when increasing the internal loss factors (ILF) of all structural elements from 0.015 to 0.12, a 13.5 dB sound insulation improvement can be observed for the 2-room system at 1000 Hz and that for the 24-room system is 10.9 dB. This method serves as a promising way to investigate the acoustic transmission in heavily damped periodic box-like structures.

Article Highlights

- A fast SEA model building method is proposed.
- A 3D coordinate based numbering system is developed for subsystem location and identification.
- Application of damping on structural elements results in better sound insulation.

Keywords Periodic box-like system · Statistical energy analysis · Acoustic modelling · Vibration prediction · Computational simulation

1 Introduction

In many practical cases, the system of interest consists of cellular units formed by plates or beams at rectangular intervals. This kind of structure, which can be seen as a periodic box-like structure, is commonly found in hotels, residences, cabins, train carriages, etc. The acoustic simulation of such systems is thus of importance either in the design stage or in the reconstruction stage to meet the noise control regulation.

The analysis of vibroacoustic problems in periodic structures has been extensively studied in the past century while using SEA. A detailed history review of applying periodic structure theory in solving wave propagation problems was given by Brillouin [1]. Mead was considered to be the first to apply periodic structure theory in analysing continuous systems [2]. Later, Keane and Price's study

✉ Feng Yan, yanfeng1988@tzc.edu.cn | [1]Taizhou University, NO. 1139 Shi Fu Da Dao, Jiaojiang, Taizhou 318000, Zhejiang, China. [2]University of Nottingham, Nottingham, UK.

extended the use of periodic structure theory to SEA and showed better energy flow predictions than traditional SEA between two parts of a ship's structure [3].

Standard SEA has been widely used in predicting mid and high frequency vibrational energy transmission in complex systems such as buildings, automobiles, ships, satellites, etc. [4]. The basic idea behind SEA is to divide the building into subsystems (usually but not always to represent the physical elements such as walls, floors, ceilings, etc. and the rooms they enclose) and assumes the energy only flows from one subsystem to neighbouring subsystems (there are exceptions, such as non-resonant transmission). To be more specific, a subsystem is an acoustic space or a structure that consists of a group of similar resonant modes [5]. The SEA framework assumes that the energy in each subsystem is contained in resonant modes so that the energy is proportional to the damping. There are cases where the response of an element is not proportional to the damping, which is often referred to as non-resonant transmission. Non-resonant transmission is sometimes of importance and can usually be modelled either as direct coupling between two resonant systems bypassing the physical element through which the sound is passing non-resonantly or by introducing additional noise sources [4]. The energy flows between subsystems are represented by the coupling loss factor (CLF). Modal density is generally considered as an indicator to determine whether a system is suitable for SEA modelling. Langley derived the general expressions for the modal density of one- and two-dimensional periodic structures based on periodic structure theory [6]. Langley et al. further discussed the high-frequency vibration transmission through a stiffened panel where periodic structure theory is used to compute the transmission and absorption coefficients [7]. Craik investigated the contribution of long flanking transmission in periodic box-like systems using SEA [12]. Recently, Wilson and Hopkins discussed the effects of spatial filtering of three-dimensional periodic box-like structures using Advanced SEA (ASEA) [8]. Andrade et al. experimentally validated the high frequency SEA prediction of the variance of energy in coupled structural–acoustic systems [18]. Yan et al. examined the damping effect of 9 different periodic box-like structures using SEA [9]. Poblet-Puig discussed the CLFs of L, T, and X-junctions for both out-of-plane and in-plane waves as well as their interactions [19]. These types of junctions are very common in periodic box-like structures. Unfortunately, although the underlying theories were explained in the aforementioned studies, details of the model building were not very specific. Efforts have been done in order to help in the creation of SEA models [15–17]. Most of them try to be general-purpose methods not designed with the goal to be applied to a single geometry type.

In many cases, the structural element in periodic box-like structures can have very high damping levels with various passive damping treatments. In such cases, the energy attenuation along transmission paths within the structural elements becomes very significant, violating the basic SEA assumption, i.e., a diffused field. When the energy distribution within a structural element is no longer diffused, this element can no longer be seen as a subsystem. The authors proposed a hybrid Ray-Tracing-SEA method to investigate the acoustic transmission in a five-plate system and a one-room system [13, 14]. The energy transmission across heavily-damped structural elements was computed with a forward ray-tracing method and represented using 'equivalent CLFs'. The hybrid models were built where heavily-damped elements were treated as 'coupling elements'. It is found that with the increasing number of damped elements and the value of damping level, the direct path tends to dominate the transmission, and the prediction from classic SEA becomes less accurate. Unfortunately, this finding is limited to simple models at the moment. To further understand the influence of damping treatment in more complicated periodic box-like structures, one needs to develop a simple model building method that can create, locate, and change structures. Although previous studies have shown great insight in understanding the principles of vibroacoustic transmission in periodic structures, few attempts are made for fast model building.

In this paper, the authors intended to propose an algorithm for fast SEA model building for periodic box-like structures. The rationale of the algorithm is given in the next section. Validation and a numerical study of two models are followed. The limitation of the proposed method is also discussed. A sample script is presented in the Appendix.

2 Fast SEA model building

2.1 Classic SEA modelling

In classic SEA modelling, the proportion of energy transmitted from subsystem *i* to subsystem *j* in one-radian cycle is called the coupling loss factor (CLF), denoted as η_{ij}. The proportion of energy that is dissipated as heat per radian cycle within subsystem *i* is called the internal loss factor (ILF), denoted as η_{id}. The sum of the CLFs and the ILF of subsystem *i* is called the total loss factor (TLF), denoted as η_i, which represents the proportion of the total energy leaving the subsystem per radian cycle. The energy of subsystem *i*, denoted as E_i, can be readily found with known energy input through the classic matrix:

$$\begin{bmatrix} -\eta_1 & \eta_{21} & \eta_{31} & \cdots & \eta_{N1} \\ \eta_{12} & -\eta_2 & \eta_{32} & & \\ \eta_{13} & \eta_{23} & -\eta_3 & & \\ \vdots & & \ddots & & \\ \eta_{1N} & & & & -\eta_N \end{bmatrix} \begin{bmatrix} E_1 \\ E_2 \\ E_3 \\ \vdots \\ E_N \end{bmatrix} = \begin{bmatrix} -W_1/\omega \\ -W_2/\omega \\ -W_3/\omega \\ \vdots \\ -W_N/\omega \end{bmatrix} \quad (1)$$

where W_i represents the energy input of subsystem i and ω is the angular frequency. All the TLFs and CLFs in the matrix above can be determined theoretically or experimentally [4]. With the aid of SEA modelling software, such as the commercial software VAone (SEA module), AutoSEA, or the Parallel Programmable Calculator (PPC) written by Craik (2011) [10], the energy distribution through the system can be obtained once the model has been established. The most time-consuming part of SEA analysis usually is model building, i.e., specifying the property of each subsystem and how they are connected. For commercial SEA software, such as VAone, the source code is usually closed, limiting the possibility of modifying specific calculations. There are four common methods of SEA model creation: 1) specifying node locations—creating subsystems – specifying connectivity – creating SEA model (VAone); 2) creating subsystems with templates – specifying connectivity – creating SEA model (PPC, VAone); 3) importing CAD geometry – creating finite element faces – creating SEA model (VAone); 4) creating SEA model from a script (PPC, VAone). The first two methods generate SEA models manually. The third method is typically useful for very complex systems such as ships, submarines, cars, etc. The last method provides freedom and automatization to create SEA models. Normally, each subsystem is auto-assigned a number, which usually starts from 1. The assigned number does not have any physical meaning. As the complexity of the model grows, it is relatively harder to locate a specific subsystem by checking the name of each subsystem. In the case of studying heavily damped systems, one needs to precisely locate and change the properties of different elements. This requires a new naming system of the SEA model. In addition, as the damping level gets higher, the predicting results from classic SEA tend to be inaccurate [13, 14] and refined SEA models need to be built. The proposed method is typically useful in such kind of study.

A typical one-room system is shown in Fig. 1. It consists of 6 structural subsystems and 1 cavity (room). The illustration of the corresponding SEA model is shown in Fig. 2, where each block is assigned a number and represents one subsystem. Assuming only bending wave transmission is considered, one needs to specify the properties of 7 subsystems and 36 physical couplings between different subsystems for this typical one-room system. When adding another room, one may have a two-room system as

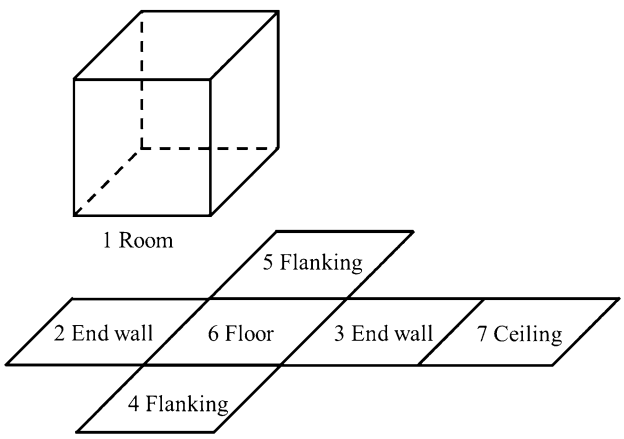

Fig. 1 Exploded view of a system consisting of one room

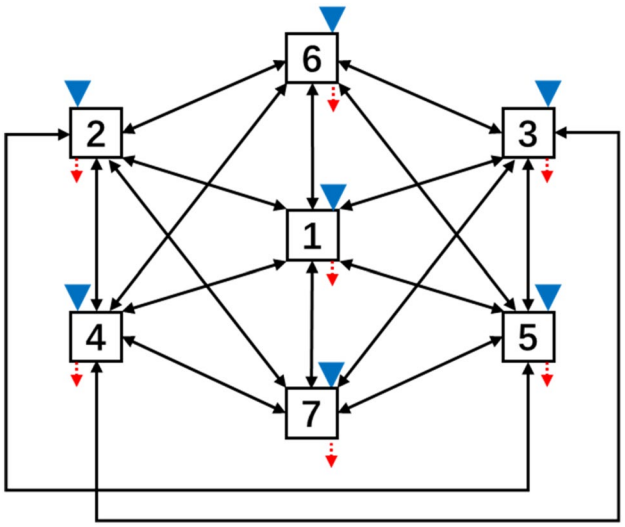

Fig. 2 The SEA model of the system shown in Fig. 1 (The blue arrows represent power inputs, the black arrows represent power flows between different subsystems through couplings, and the red arrows represent the powers dissipated due to internal damping)

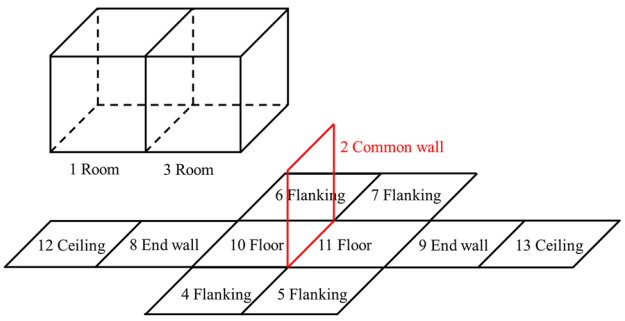

Fig. 3 Exploded view of a system consisting of two rooms separated by a common wall

shown in Fig. 3. The corresponding SEA model is shown in Fig. 4. For this system, the properties of 13 subsystems and 76 physical couplings need to be specified. In both cases, the couplings between subsystems that are not physically connected are assumed to be neglectable and are hidden from the illustrations. This requires additional time effort. For a three-wave model, a structural element supporting bending, longitudinal and transverse modes will generally need three subsystems to describe it, making the modelling even more complicated [4].

From the SEA matrix (Eq. 1), to compute the energy distribution with N subsystems, one generally needs to specify the $N \times N$ loss factor matrix and the $N \times 1$energy input matrix. As the number of subsystems grows, the model complexity increases dramatically. The common way of creating a SEA model is either using an interactive graphical interface built-in in a commercial SEA software or using a programming language. Using algorithms to build the SEA model seems to be more effective, especially for periodic box-like systems since they are orderly connected. Any further modifications of the SEA model can be readily done after the prototype model is constructed.

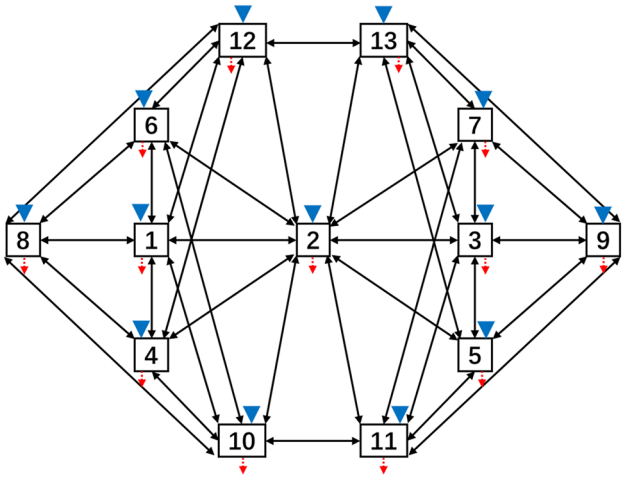

Fig. 4 The SEA model of the system shown in Fig. 3 (The blue arrows represent power inputs, the black arrows represent power flows between different subsystems through couplings, and the red arrows represent the powers dissipated due to internal damping)

2.2 General procedure of fast SEA model building

The general procedure of fast SEA model building by an algorithm is shown in Fig. 5. It consists of four steps, namely (1) numbering of subsystems and joints (couplings), (2) specifying the properties of subsystems, joints, and power input, (3) computing loss factor matrix and power input matrix, and (4) solving SEA matrix to get the energy of each subsystem. This paper proposed a novel numbering system for a periodic box-like system by placing the system in a 3D Cartesian coordinate. Step 2 can be readily done once all subsystems and joints are numbered and located. Step 3 and Step 4 can then be conducted by the SEA modelling software PPC. This algorithm works for both bending-only and three-way analysis. Although the algorithm is written solely for periodic box-like structures, the idea of subsystems and couplings numbering may be adopted in systems that are not orderly constructed.

2.3 Numbering of room subsystems

A new naming system is proposed for fast SEA model building. Taking a 4-room system (Fig. 6) as an example, if one introduces a Cartesian coordinate system into this model and uses a, b, and c to define the total number of columns, rows, and floors of the building, one may express this system as a 2*2*2 system. One may use l, w, and h to

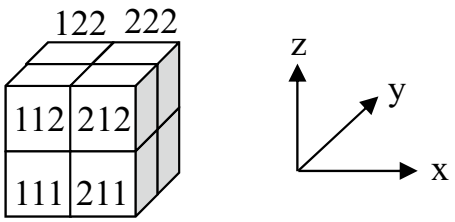

Fig. 6 Illustration of a 4-room system with a Cartesian coordinate (the following illustrations are placed in the same coordinate system)

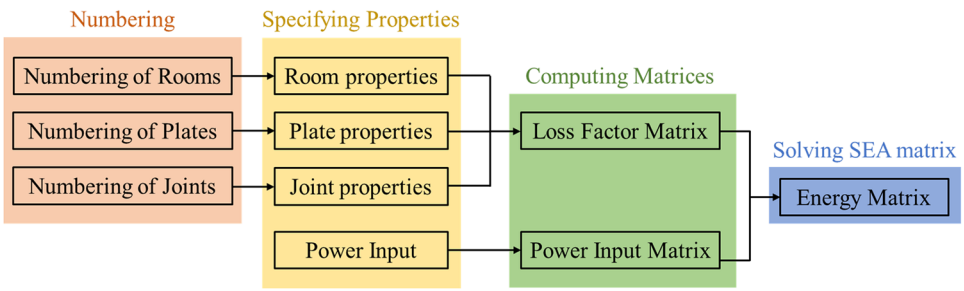

Fig. 5 Illustration of the general procedure of fast SEA model building

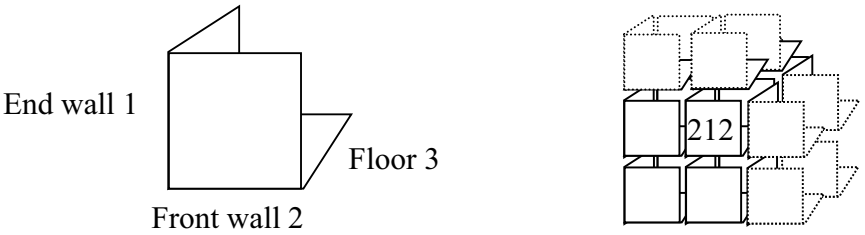

Fig. 7 Illustration of the 2*2*2 building with the basic unit

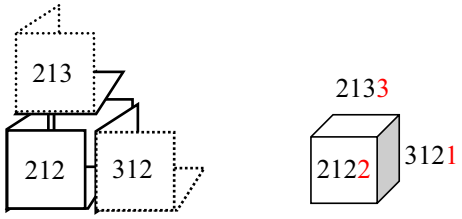

Fig. 8 Illustration of the partial components of room 212

define each room's length, width, and height, assuming all the rooms have the same dimension. By further using x, y, and z to define where the room is located among those columns, rows, and floors, respectively, the coordinate of each room can be readily determined. For example, the room in column 1, row 1, and floor 1 can be expressed as (1,1,1). One may use the number 111 to represent this room. Generally speaking, any room in this study can be numbered using $100 * x + 10 * y + z$.

2.4 Numbering of plate subsystems

One may use the basic unit shown in Fig. 7 to form the 2*2*2 building. It consists of three parts, i.e., the end wall, the front wall, and the floor. The first step of naming is to find which room those three plates belong to and then times the room number with 10 and plus 1 or 2 or 3, respectively. The unit with solid lines is real, and that with dot lines is an imaginary unit of which only one plate is real.

Therefore, each plate of this building is assigned a specific number. For example (Fig. 8), room 212 consists of 2121 (end wall of room 212), 2122 (front wall of room 212), 2123 (floor of room 212), 3121(end wall of the imagined room 312), 2222 (front wall of room 222) and 2133 (floor of the imagined room 213).

2.5 Numbering of joints

The next step is to define the joints. In periodic box-like buildings, the common joints are Cross, Tee, and Corner

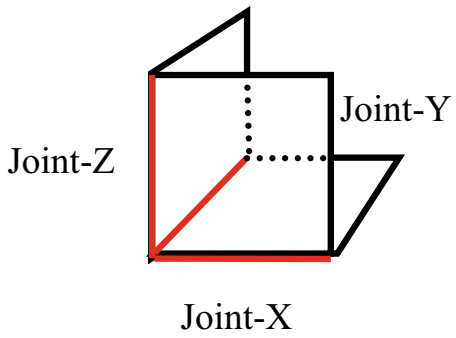

Fig. 9 Illustration of three types of joints in the basic unit

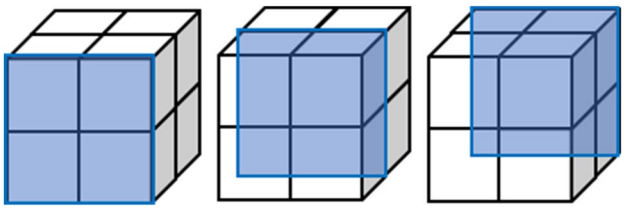

Fig. 10 Illustration of the slicing the system with the X–Z plane

joints. SEA modelling requires specifying the connection between different plates, i.e., how different plate subsystems are connected through joints. The information about the geometry and material properties is stored when the room and plate subsystems are defined. Therefore, the task remained is to specify the components of each joint.

One may use the basic unit again to define the number of each joint (Fig. 9). The joints can be categorized into three types, namely Joint-X, Joint-Y, and Joint-Z. The joint number is simply 10 times the room number and plus 10,000 or 20,000 or 30,000 respectively. Again, imaginary rooms are used.

2.5.1 Numbering of Joint-X joints

To define all Joint-X joints, one may slice the system with the X–Z plane (Fig. 10).

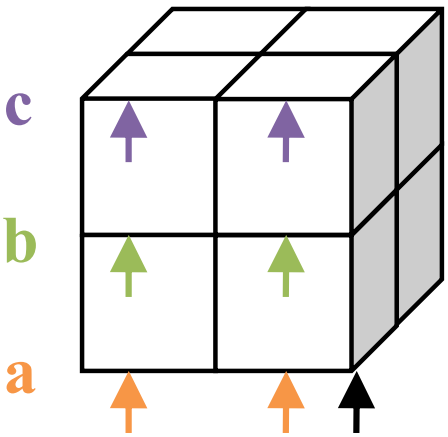

Fig. 11 Illustration of the Joint-X joints when $y = 1$

When $y = 1$, the joints at the ground floor are corner joints (Fig. 11, joints a). The number assigned to such kinds of joints is calculated through $10000 + 1000 * x + 100 + 10$ and it consists of two plates, i.e. plate $1000 * x + 100 + 10 + 2$ and plate $1000 * x + 100 + 10 + 3$. In the following content, the following expression will be used to demonstrate the joint number (equation before the bracket) and the components of that joint (equations after the bracket). Two components suggest a Corner joint, three components suggest a Tee joint, and four components suggest a Cross joint.

$$10000 + 1000 * x + 100 + 10\begin{cases} 1000 * x + 100 + 10 + 2 \\ 1000 * x + 100 + 10 + 3 \\ 0 \\ 0 \end{cases} \tag{2}$$

When $y = 1$, the joints at floors in between are tee joints (Fig. 11, joints b). The joint numbers and their components are

$$10000 + 1000 * x + 100 + 10 * z\begin{cases} 1000 * x + 100 + 10 * z + 2 \\ 1000 * x + 100 + 10 * z + 3 \\ 1000 * x + 100 + 10 * (z-1) + 2 \\ 0 \end{cases} \tag{3}$$

When $y = 1$, the joints at the top ceiling are also corner joints (Fig. 11, joints c), where

$$10000 + 1000 * x + 100 * y + 10 * (c+1)\begin{cases} 1000 * x + 100 * y + 10 * (c+1) + 3 \\ 1000 * x + 100 * y + 10 * c + 2 \\ 1000 * x + 100 * (y-1) + 10 * (c+1) + 3 \\ 0 \end{cases} \tag{7}$$

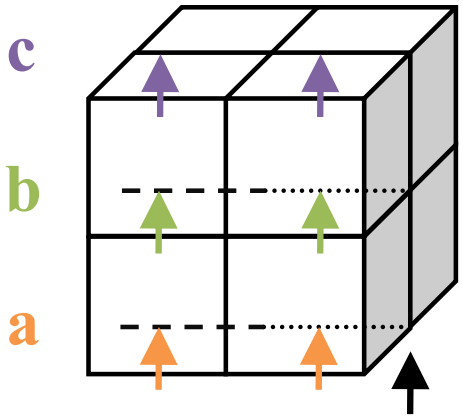

Fig. 12 Illustration of the Joint-X joints when $y = 2$ (for more general cases when $2 \le y < b + 1$)

$$10000 + 1000 * x + 100 + 10(c+1)\begin{cases} 1000 * x + 100 + 10(c+1) + 3 \\ 1000 * x + 100 + 10 * c + 2 \\ 0 \\ 0 \end{cases} \tag{4}$$

When $y = 2$, the joints at the ground floor are tee joints (Fig. 12, joints a). For more general cases, when $2 \le y < b + 1$, one has

$$10000 + 1000 * x + 100 * y + 10\begin{cases} 1000 * x + 100 * (y-1) + 10 + 3 \\ 1000 * x + 100 * y + 10 + 2 \\ 1000 * x + 100 * y + 10 + 3 \\ 0 \end{cases} \tag{5}$$

When $2 \le y < b + 1$, the joints at the floors in between are cross joints (Fig. 12, joints b), where

$$10000 + 1000 * x + 100 * y + 10 * z\begin{cases} 1000 * x + 100 * y + 10 * z + 2 \\ 1000 * x + 100 * y + 10 * z + 3 \\ 1000 * x + 100 * y + 10 * (z-1) + 2 \\ 1000 * x + 100(y-1) + 10 * z + 3 \end{cases} \tag{6}$$

When $2 \le y < b + 1$, the joints at the top ceiling are also tee joints (Fig. 12, joints c), where

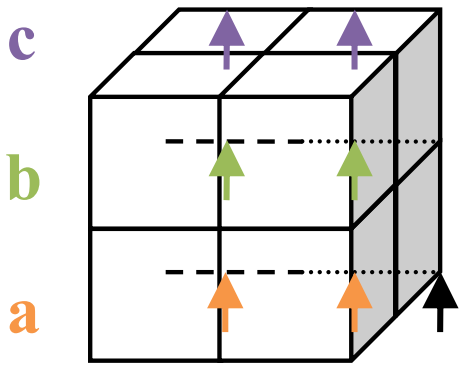

Fig. 13 Illustration of the Joint-X joints when $y = b + 1$

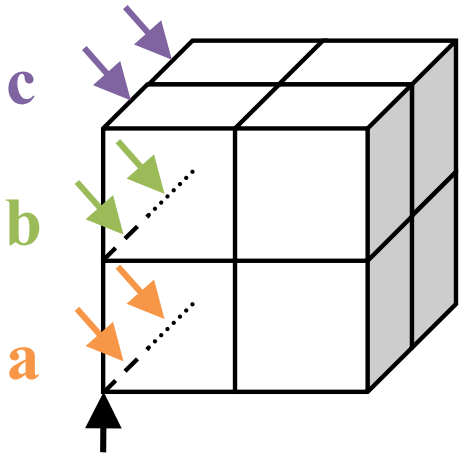

Fig. 14 Illustration of the Joint-Y joints when $x = 1$

When $y = b + 1$ (in this case $y = 3$), the joints at the ground floor are corner joints (Fig. 13, joints a). They are actually the Joint-X joints of the imagined rooms, where

$$10000 + 1000 * x + 100 * (b + 1) + 10\begin{cases} 1000 * x + 100 * b + 10 + 3 \\ 1000 * x + 100 * (b + 1) + 10 + 2 \\ 0 \\ 0 \end{cases} \tag{8}$$

When $y = b + 1$, the joints at the floors in between are tee joints (Fig. 13, joints b), where

$$10000 + 1000 * x + 100 * (b + 1) + 10 * z\begin{cases} 1000 * x + 100 * (b + 1) + 10 * (z - 1) + 2 \\ 1000 * x + 100 * b + 10 * z + 3 \\ 1000 * x + 100 * (b + 1) + 10 * z + 2 \\ 0 \end{cases} \tag{9}$$

When $y = b + 1$, the joints at the top ceiling are corner joints (Fig. 13, joints c), where

$$10000 + 1000 * x + 100 * (b + 1) + 10(c + 1)\begin{cases} 1000 * x + 100 * (b + 1) + 10 * c + 2 \\ 1000 * x + 100 * b + 10(c + 1) + 3 \\ 0 \\ 0 \end{cases} \tag{10}$$

2.5.2 Numbering of Joint-Y joints

To define all Joint-Y joints, one may slice the building with the Y–Z plane.

When $x = 1$, the joints at the ground floor are corner joints (Fig. 14, joints a), where

$$20000 + 1000 + 100 * y + 10\begin{cases} 1000 + 100 * y + 10 + 1 \\ 1000 + 100 * y + 10 + 3 \\ 0 \\ 0 \end{cases} \tag{11}$$

When $x = 1$, the joints at the floors in between are tee joints (Fig. 14, joints b), where

$$20000 + 1000 + 100 * y + 10 * z \begin{cases} 1000 + 100 * y + 10 * z + 1 \\ 1000 + 100 * y + 10 * z + 3 \\ 1000 + 100 * y + 10(z-1) + 1 \\ 0 \end{cases} \tag{12}$$

When $x = 1$, the joints at the top ceiling are corner joints (Fig. 14, joints c), where

$$20000 + 1000 * x + 100 * y + 10 * z \begin{cases} 1000 * x + 100 * y + 10 * z + 1 \\ 1000 * x + 100 * y + 10 * z + 3 \\ 1000 * x + 100 * y + 10(z-1) + 1 \\ 1000(x-1) + 100 * y + 10 * z + 3 \end{cases} \tag{15}$$

$$20000 + 1000 + 100 * y + 10(c+1) \begin{cases} 1000 + 100 * y + 10(c+1) + 3 \\ 1000 + 100 * y + 10 * c + 1 \\ 0 \\ 0 \end{cases} \tag{13}$$

When $2 \leq x < a + 1$(in this case $x = 2$), the joints at the ground floor are tee joints (Fig. 15, joints a), where

$$20000 + 1000 * x + 100 * y + 10 \begin{cases} 1000(x-1) + 100 * y + 10 + 3 \\ 1000 * x + 100 * y + 10 + 1 \\ 1000 * x + 100 * y + 10 + 3 \\ 0 \end{cases} \tag{14}$$

When $2 \leq x < a + 1$, the joints at floors in between are cross joints (Fig. 15, joints b), where

When $2 \leq x < a + 1$, the joints at the top ceiling are tee joints (Fig. 15, joints c), where

$$20000 + 1000 * x + 100 * y + 10(c+1) \begin{cases} 1000 * x + 100 * y + 10(c+1) + 3 \\ 1000 * x + 100 * y + 10 * c + 1 \\ 1000(x-1) + 100 * y + 10(c+1) + 3 \\ 0 \end{cases} \tag{16}$$

When $x = a + 1$ (in this case $x = 3$), the joints at the ground floor are corner joints (Fig. 16, joints a), where

$$20000 + 1000(a+1) + 100 * y + 10 \begin{cases} 1000 * a + 100 * y + 10 + 3 \\ 1000(a+1) + 100 * y + 10 + 1 \\ 0 \\ 0 \end{cases} \tag{17}$$

When $x = a + 1$, the joints at floors in between are tee joints (Fig. 16, joints b), where

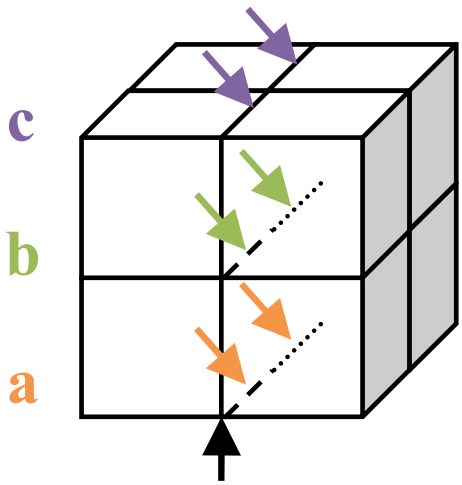

Fig. 15 Illustration of the Joint-Y joints when $2 \leq x < a + 1$

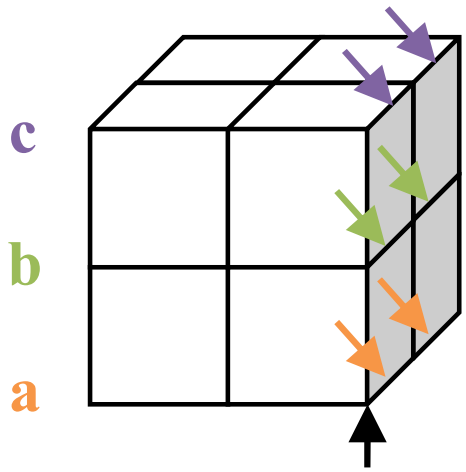

Fig. 16 Illustration of the Joint-Y joints when $x = a + 1$

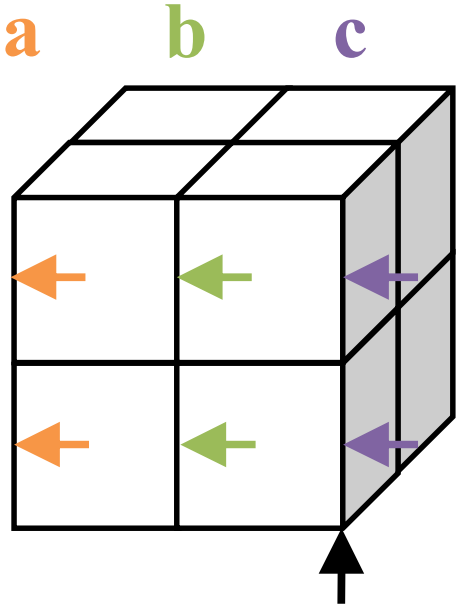

Fig. 17 Illustration of the Joint-Z joints when $y = 1$

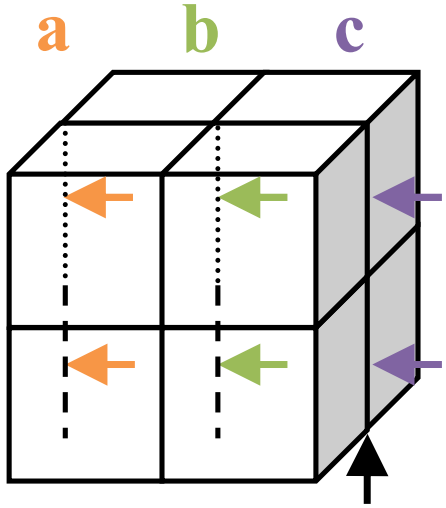

Fig. 18 Illustration of the Joint-Z joints when $2 \leq y < b + 1$

$$20000 + 1000(a+1) + 100 * y + 10 * z \begin{cases} 1000(a+1) + 100 * y + 10(z-1) + 1 \\ 1000 * a + 100 * y + 10 * z + 3 \\ 1000(a+1) + 100 * y + 10 * z + 1 \\ 0 \end{cases} \tag{18}$$

When $x = a + 1$, the joints at the top ceiling are corner joints (Fig. 16, joints c), where

$$20000 + 1000(a+1) + 100 * y + 10(c+1) \begin{cases} 1000(a+1) + 100 * y + 10 * c + 1 \\ 1000 * a + 100 * y + 10(c+1) + 3 \\ 0 \\ 0 \end{cases} \tag{19}$$

2.5.3 Numbering of Joint-Z joints

To define all Joint-Z joints, one may slice the building with the X–Z plane.

When $y = 1$, the joints of the left end walls of the building are corner joints (Fig. 17, joints a), where

$$30000 + 1000 + 100 + 10 * z \begin{cases} 1000 + 100 + 10 * z + 1 \\ 1000 + 100 + 10 * z + 2 \\ 0 \\ 0 \end{cases} \tag{20}$$

When $y = 1$, the joints of the common end walls are tee joints (Fig. 17, joints b), where

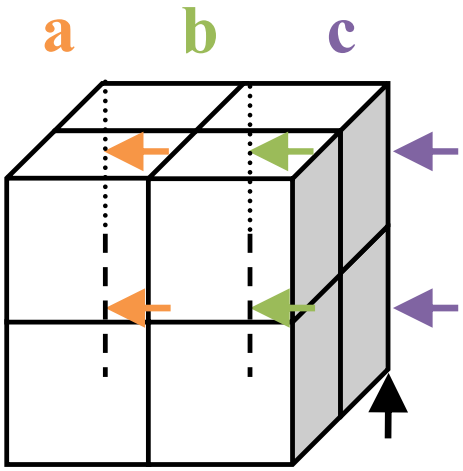

Fig. 19 Illustration of the Joint-Z joints when $y = b + 1$

$$30000 + 1000 * x + 100 + 10 * z \begin{cases} 1000(x-1) + 100 + 10 * z + 2 \\ 1000 * x + 100 + 10 * z + 1 \\ 1000 * x + 100 + 10 * z + 2 \\ 0 \end{cases} \quad (21)$$

When $y = 1$, the joints of the right end walls of the building are corner joints (Fig. 17, joints c), where

$$30000 + 1000(a+1) + 100 + 10 * z \begin{cases} 1000 * a + 100 + 10 * z + 2 \\ 1000(a+1) + 100 + 10 * z + 1 \\ 0 \\ 0 \end{cases} \quad (22)$$

When $2 \leq y < b + 1$(in this case $y = 2$), the joints of the left end walls of the building are tee joints (Fig. 18, joints a), where

$$30000 + 1000 + 100 * y + 10 * z \begin{cases} 1000 + 100 * y + 10 * z + 1 \\ 1000 + 100 * y + 10 * z + 2 \\ 1000 + 100(y-1) + 10 * z + 1 \\ 0 \end{cases} \quad (23)$$

When $2 \leq y < b + 1$, the joints of the common end walls are cross joints (Fig. 18, joints b), where

$$30000 + 1000 * x + 100 * y + 10 * z \begin{cases} 1000 * x + 100 * y + 10 * z + 1 \\ 1000 * x + 100 * y + 10 * z + 2 \\ 1000 * x + 100(y-1) + 10 * z + 1 \\ 1000(x-1) + 100 * y + 10 * z + 2 \end{cases} \quad (24)$$

When $2 \leq y < b + 1$, the joints of the right end walls of the building are tee joints (Fig. 18, joints c), where

$$30000 + 1000(a+1) + 100 * y + 10 * z \begin{cases} 1000(a+1) + 100(y-1) + 10 * z + 1 \\ 1000 * a + 100 * y + 10 * z + 2 \\ 1000(a+1) + 100 * y + 10 * z + 1 \\ 0 \end{cases} \quad (25)$$

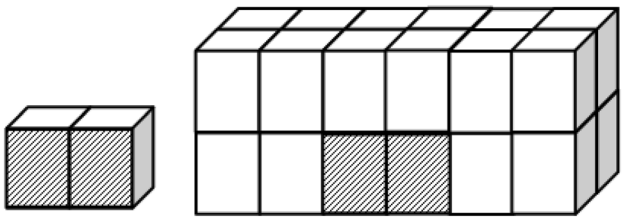

Fig. 20 Illustration of a simple 2-room system and a complicated 24-room system (the shadowed rooms are the source room and the receiving room)

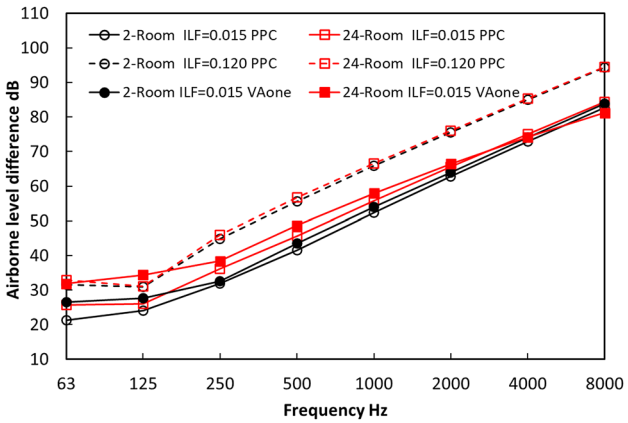

Fig. 21 Air-borne energy level differences between the source room and the receiving room for simple and complicated system predicted by VAone and PPC

Table 1 Dimensions and material properties of the systems in Fig. 19

Element	Room	Common wall	Other wall	Floor
Dimensions (m)	3×4×2.5	3×2.5	3 or 4×2.5	3×4
Material		Brick	Brick	Concrete
Thickness (m)		0.2	0.1	0.15
Density (kg/m^3)		2000	2000	2300
Longitudinal wave speed (m/s)		2000	2000	3400
Critical frequency (Hz)		162	324	127
Poisson's ratio		0.2	0.2	0.2
Initial internal loss factor		0.015	0.015	0.015
Reverberation time (s)	0.5			

When $y = b + 1$(in this case $y = 3$), the joints of the left end walls of the building are corner joints (Fig. 19, joints a), where

$$30000 + 1000 + 100(b+1) + 10 * z \begin{cases} 1000 + 100(b+1) + 10 * z + 2 \\ 1000 + 100 * b + 10 * z + 1 \\ 0 \\ 0 \end{cases} \tag{26}$$

When $y = b + 1$, the joints of the common end walls are tee joints (Fig. 19, joints b), where

$$30000 + 1000 * x + 100(b+1) + 10 * z \begin{cases} 1000 * x + 100(b+1) + 10 * z + 2 \\ 1000 * x + 100 * b + 10 * z + 1 \\ 1000(x-1) + 100(b+1) + 10 * z + 2 \\ 0 \end{cases} \tag{27}$$

When $y = b + 1$, the joints of the right end walls of the building are corner joints (Fig. 19, joints c), where

$$30000 + 1000(a+1) + 100(b+1) + 10 * z \begin{cases} 1000(a+1) + 100 * b + 10 * z + 1 \\ 1000 * a + 100(b+1) + 10 * z + 2 \\ 0 \\ 0 \end{cases} \tag{28}$$

2.6 Fast SEA modelling

When all the subsystems and their connections are specified, with the aid of SEA modelling software PPC, acoustic analysis of common periodic box-like buildings can be conducted straightaway. In PPC, there is a built-in function to change the bending-only model to the three-wave model. It is relatively simple to change the properties of subsystems and joints using the numbering system proposed. This serves as a promising way of studying the effect of changing the properties of different subsystems and path sensitivity analysis such as the contribution from flanking transmission. Typically, studies about acoustic transmission in heavily-damped systems with repeatable patterns can benefit from this method. To check the validity of the proposed method, a simple 2-room system and a complicated 24-room system (Fig. 20) were built manually and automatically in PPC. Both methods gave identical models. Three attempts were conducted to decrease the model building time through improved proficiency but the effect was quite limited. The average time used to build the two models manually was 6 min 37 s and 41 min 12 s respectively. The model building time of the proposed method was less than 1 min for both models. It took additional 15 s for the computer to compute the 24-room system. If one is interested in changing the dimension or coupling type, there are two options. One may either change the relevant parameters in the script and regenerate the model (less than 1 min) or use the built-in functions in PPC to change it (normally more than 1 min). To further validate the proposed method, comparisons to the commercial software VAone are conducted in the following section.

3 Validation and application of the fast SEA modelling method

Validation is conducted by comparing the modelling results between manually-built SEA models in VAone software and script-generated SEA models in PPC for 2-Room system and 24-Room system (Fig. 20). The model information assumed is shown in Table 1. A trial prediction has been conducted to show no significant difference between bending-only and three-wave models. The prediction results from bending transmission are demonstrated.

The predictions from the models generated by the proposed algorithm generally show similar results to those from VAone simulation (Fig. 21), except it only took 1 min to build the models with the script and half an hour to create manually. Divergency is found at the lower frequency range (below 250 Hz). One possible explanation is that VAone and PPC use different expressions to compute coupling loss factors. The modeling of PPC is based on Robert J.M. Craik's book on 'Sound transmission through buildings

using Statistical Energy Analysis' [4]. Unfortunately, the authors could not find the expressions for coupling loss factors in VAone as the source code is closed. This is the exact drawback of the 'black-box' effect of commercial software as discussed in Sect. 2.1. For the studied systems at frequencies below 250 Hz, the mode count N is less than 4.4 and the modal overlap M is less than 5.5. As Hopkins suggested, one condition for SEA to be 'appropriate' for plates is $N \geq 5$ and $M \geq 1$[11]. Therefore, the validity of the prediction below 250 Hz is questionable and the results at frequencies above 250 Hz are valid.

Assuming one interests in finding the acoustic benefit of increasing the internal damping of the two systems shown in Fig. 20. With the assistance of the fast SEA modelling script, the complicated system can be built and analysed with simplicity. When the internal loss factor of each structural subsystem is increased from 0.015 to 0.120 by applying passive damping treatment, the air-borne energy level differences between the source room and the receiving room are shown in Fig. 21. In this analysis, the internal loss factor has been increased to a very high level for demonstration purposes. In practical cases, concrete walls can rarely reach such a high damping level, while it is possible for metal plates using constrained layer damping. This analysis shows the potential acoustic benefit of applying damping treatment in structural elements in periodic box-like structures.

When both systems are undamped, the energy level difference between the source and receiving rooms is 52.3 dB and 55.7 dB for the simple and complicated systems at 1000 Hz, respectively. The 24-room system, i.e., system with more structural subsystems, appears to have better sound insulation than the 2-room system because there are more structures for sound to travel into and be attenuated before arriving in the receiving room. When both systems are damped, one observes a 13.5 dB sound insulation increase for the simple system at 1000 Hz and a 10.9 dB increase for the complicated one. This suggests that the application of damping treatment is more beneficial for systems with fewer structural elements. Another interesting finding is that both systems have almost the same sound reduction when the damping level is high. With a high damping level, the contribution of flanking transmission (especially long flanking path) is small, and the transmission is dictated by the direct path. These findings also agree with previous work done by Craik [12] and Yan [9]. Once the SEA model has been established, the air-borne energy level difference between any two rooms and the energy level difference between any two subsystems can be predicted. Path sensitivity analysis can also be carried out to check the contribution of different paths. Further investigation about the sound insulation benefit caused by increasing damping will not be conducted as it is beyond the scope of this paper.

The proposed method is essential in the evaluation of the vibroacoustic problems in heavily-damped periodic box-like systems. As the damping levels of structural elements increase, the basic SEA assumption of energy equipartition tends to fail. Previous studies have shown that in such cases, classic SEA tends to give unreliable results and needs modifications [13, 14]. One way to overcome the induced problem is to modify the SEA model with equivalent CLF. The proposed method is applicable in such a case.

4 Limitations

This work intends to provide a way to fast create a base SEA model and understand the benefit brought by increasing the damping levels of structural elements. One contribution of this work is the idea of relating the names of subsystems with geometric meaning. The studied numerical models are ideal with many simplifications, i.e., omitting windows and doors. Further refining of the model, such as adding holes or ventilation systems, could be done to study a more realistic model but is beyond our current research goal and needs future effort.

Another limitation of the proposed method is that if one needs to add or delete a structural element once the system has been built, it requires an additional step, and the naming system is challenged in such a case. Adding or deleting subsystems can be realized in the software with a built-in function. One possible way to overcome the problem brought by adding or deleting subsystems is to give new numbers locally, i.e., only changing the names of connected subsystems and keeping the names of the rest of the subsystems.

5 Conclusions

A fast Statistical Energy Analysis modelling method is introduced by using a new numbering system to define subsystems and joints of periodic box-like buildings. It greatly increases the efficiency of SEA modelling and provides a fast way of analysing complicated systems.

The study of two numerical systems suggests that a system with more structural elements usually has better sound insulation than the one with fewer structural elements. The applications of damping treatment result in more significant acoustic benefits for the latter one. When both systems are damped, there is a similar energy level difference between the source and the receiving room.

The study of this paper serves as a starter of fast SEA modelling for complicated systems, especially for systems with heavily-damped structures. It enables the model builder to precisely locate and make the modification of

each subsystem's SEA parameter, i.e., the modal density, the bending wave speed, the bending wave number, the bending wavelength, the damping loss factor, and the critical frequency. The proposed method is limited to periodic box-like systems, but it shows the potential to contribute to vibroacoustic modelling of systems with repeatable patterns. Future work is needed to extend its application to more general systems, including structural elements in different shapes (i.e., curved plate, cylinder, etc.).

Funding This research was supported in part by the Natural Science Foundation of Zhejiang Province under Grant Number LQ18E080003.

Data availability The datasets generated during and/or analysed during the current study are available from the corresponding author on reasonable request.

Declarations

Conflict of interests The authors declare that there is no conflict of interest associated with the subject of the article.

Appendix

The sample script of a 6*2*2 building is demonstrated here for readers with further interest. This script is based on the C language and works in PPC. It provides a fast way to create a base model which can later be modified. Although it can not be directly used in other software, the authors hope it could benefit the acoustic community to some extent. The use of '$' before variables is required by the default setting in PPC. This does not follow conventional standards in typesetting mathematical texts and is addressed here.

```
isystem 3 9 4 2
        4 2 2
        0 10 1 0 10000
$a=6 $b=2 $c=2 $l=4 $w=3 $h=2.5 $i=0.015 $r=0.5 for $x 1 1 $a for $y 1 1 $b for $z 1 1 $c isubsystem [100 $x * 10 $y * + $z +] 1 $l $w $h $r /* room */
for $x 1 1 $a for $y 1 1 $b for $z 1 1 $c isubsystem [1000 100 $y * + 10 $z * + 1 +] 2 $w $h 0.1 2 2000 0.2 2 324 $i /* Plate */
for $x 2 1 $a for $y 1 1 $b for $z 1 1 $c isubsystem [1000 $x * 100 $y * + 10 $z * + 1 +] 2 $w $h 0.2 2 2000 0.2 2 162 $i /* Plate */
for $x 1 1 $a for $y 1 1 $b for $z 1 1 $c isubsystem [$a 1 + 1000 * 100 $y * + 10 $z * + 1 +] 2 $w $h 0.1 2 2000 0.2 2 324 $i /* Plate */
for $x 1 1 $a for $y 1 1 $b for $z 1 1 $c isubsystem [1000 $x * 100 + 10 $z * + 2 +] 2 $l $h 0.1 2 2000 0.2 2 324 $i /* Plate */
for $x 1 1 $a for $y 2 1 $b for $z 1 1 $c isubsystem [1000 $x * 100 $y * + 10 $z * + 2 +] 2 $l $h 0.1 2 2000 0.2 2 324 $i /* Plate */
for $x 1 1 $a for $y 1 1 $b for $z 1 1 $c isubsystem [$b 1 + 100 * 1000 $x * + 10 $z * + 2 +] 2 $l $h 0.1 2 2000 0.2 2 324 $i /* Plate */
for $x 1 1 $a for $y 1 1 $b for $z 1 1 $c isubsystem [1000 $x * 100 $y * + 10 + 3 +] 2 $l $w 0.15 2 2300 0.2 2 127 $i /* Plate */
for $x 1 1 $a for $y 1 1 $b for $z 2 1 $c isubsystem [1000 $x * 100 $y * + 10 $z * + 3 +] 2 $l $w 0.15 2 2300 0.2 2 127 $i /* Plate */
for $x 1 1 $a for $y 1 1 $b for $z 1 1 $c isubsystem [$c 1 + 10 * 1000 $x * + 100 $y * + 3 +] 2 $l $w 0.15 2 2300 0.2 2 127 $i /* Plate */
/* Input joint details */
for $x 1 1 $a for $y 1 1 $b for $z 1 1 $c $R=(1000 $x *) ijoint [$R 10110 +] [$R 112 +] [$R 113 +] 0 0 $l 1 /* Normal joint */
for $x 1 1 $a for $y 1 1 $b for $z 2 1 $c $R=(1000 $x * 10 $z * +) ijoint [$R 10100 +] [$R 102 +] [$R 103 +] [$R 92 +] 0 $l 1 /* Normal joint */
for $x 1 1 $a for $y 1 1 $b for $z 1 1 $c $R=(1000 $x * 10 $c * +) ijoint [$R 10110 +] [$R 113 +] [$R 102 +] 0 0 $l 1 /* Normal joint */
```

```
for $x 1 1 $a for $y 2 1 $b for $z 1 1 $c $R=(1000 $x * 100 $y * +) ijoint [$R 10010 +] [$R 87 -] [$R 12 +] [$R 13 +] 0 $l 1 /* Normal joint */

for $x 1 1 $a for $y 2 1 $b for $z 2 1 $c $R=(1000 $x * 100 $y * + 10 $z * +) ijoint [$R 10000 +] [$R 2 +] [$R 3 +] [$R 8 -] [$R 97 -] $l 1 /* Normal joint */

for $x 1 1 $a for $y 2 1 $b for $z 1 1 $c $R=(1000 $x * 100 $y * + 10 $c * +) ijoint [$R 10010 +] [$R 13 +] [$R 2 +] [$R 87 -] 0 $l 1 /* Normal joint */

for $x 1 1 $a for $y 1 1 $b for $z 1 1 $c $R=(1000 $x * 100 $b * +) ijoint [$R 10110 +] [$R 13 +] [$R 112 +] 0 0 $l 1 /* Normal joint */

for $x 1 1 $a for $y 1 1 $b for $z 2 1 $c $R=(1000 $x * 100 $b * + 10 $z * +) ijoint [$R 10100 +] [$R 92 +] [$R 3 +] [$R 102 +] 0 $l 1 /* Normal joint */

for $x 1 1 $a for $y 1 1 $b for $z 1 1 $c $R=(1000 $x * 100 $b * + 10 $c * +) ijoint [$R 10110 +] [$R 102 +] [$R 13 +] 0 0 $l 1 /* Normal joint */

for $x 1 1 $a for $y 1 1 $b for $z 1 1 $c $R=(10 $z *) ijoint [$R 21110 +] [$R 1101 +] [$R 1102 +] 0 0 $h 1 /* Normal joint */

for $x 2 1 $a for $y 1 1 $b for $z 1 1 $c $R=(1000 $x * 10 $z * +) ijoint [$R 20110 +] [$R 898 -] [$R 101 +] [$R 102 +] 0 $h 1 /* Normal joint */

for $x 1 1 $a for $y 1 1 $b for $z 1 1 $c $R=(1000 $a * 10 $z * +) ijoint [$R 21100 +] [$R 102 +] [$R 1101 +] 0 0 $h 1 /* Normal joint */

for $x 1 1 $a for $y 2 1 $b for $z 1 1 $c $R=(100 $y * 10 $z * +) ijoint [$R 21000 +] [$R 1001 +] [$R 1002 +] [$R 901 +] 0 $h 1 /* Normal joint */

for $x 2 1 $a for $y 2 1 $b for $z 1 1 $c $R=(1000 $x * 100 $y * + 10 $z * +) ijoint [$R 20000 +] [$R 1 +] [$R 2 +] [$R 99 -] [$R 998 -] $h 1 /* Normal joint */

for $x 1 1 $a for $y 2 1 $b for $z 1 1 $c $R=(1000 $a * 100 $y * + 10 $z * +) ijoint [$R 21000 +] [$R 901 +] [$R 2 +] [$R 1001 +] 0 $h 1 /* Normal joint */

for $x 1 1 $a for $y 1 1 $b for $z 1 1 $c $R=(100 $b * 10 $z * +) ijoint [$R 21100 +] [$R 1102 +] [$R 1001 +] 0 0 $h 1 /* Normal joint */

for $x 2 1 $a for $y 1 1 $b for $z 1 1 $c $R=(1000 $x * 100 $b * + 10 $z * +) ijoint [$R 20100 +] [$R 102 +] [$R 1 +] [$R 898 -] 0 $h 1 /* Normal joint */

for $x 1 1 $a for $y 1 1 $b for $z 1 1 $c $R=(1000 $a * 100 $b * + 10 $z * +) ijoint [$R 21100 +] [$R 1001 +] [$R 102 +] 0 0 $h 1 /* Normal joint */
```

for $x 1 1 $a for $y 2 1 $b for $z 1 1 $c clf [1000 $x * 100 $y * + 10 $z * + 2 +] [100 $x * 10 $y * + $z + 10 -] [$l $h *] [$l $h + 2 *] /* CLF room to wall */

for $x 1 1 $a for $y 1 1 $b for $z 1 1 $c clf [1000 $x * 100 $b * + 10 $z * + 102 +] [100 $x * 10 $b * + $z +] [$l $h *] [$l $h + 2 *] /* CLF room to wall */

for $x 1 1 $a for $y 1 1 $b for $z 1 1 $c clf [1000 $x * 100 $y * + 10 + 3 +] [100 $x * 10 $y * + 1 +] [$l $w *] [$l $w + 2 *] /* CLF room to wall */

for $x 1 1 $a for $y 1 1 $b for $z 2 1 $c clf [1000 $x * 100 $y * + 10 $z * + 3 +] [100 $x * 10 $y * + $z +] [$l $w *] [$l $w + 2 *] /* CLF room to wall */

for $x 1 1 $a for $y 1 1 $b for $z 2 1 $c clf [1000 $x * 100 $y * + 10 $z * + 3 +] [100 $x * 10 $y * + $z + 1 -] [$l $w *] [$l $w + 2 *] /* CLF room to wall */

for $x 1 1 $a for $y 1 1 $b for $z 1 1 $c clf [1000 $x * 100 $y * + 10 $c * + 13 +] [100 $x * 10 $y * + $c +] [$l $w *] [$l $w + 2 *] /* CLF room to wall */

joint *

dwin 311 100

ftlf

HEALTH

solve

References

1. Brillouin L (1946) Wave propagation in periodic structures. Dover, New York
2. Mead DJ (1973) A general theory of harmonic wave propagation in linear periodic systems with multiple coupling. J Sound Vib 27(2):235–260. https://doi.org/10.1016/0022-460X(73)90064-3
3. Keanew G, Price AJ (1989) Statistical energy analysis of periodic structures. Proc Royal Soc London Ser A Math Phys Sci. 423(1865):331–360
4. Craik RJM (1996) Sound transmission through buildings: using statistical energy analysis. Gower Publishing Company, Aldershot
5. Burroughs CB, Fischer RW, Kern FR (1997) An introduction to statistical energy analysis. J Acoustical Soc Am 101(4):1779–1789. https://doi.org/10.1121/1.418074
6. Langley RS (1994) On the modal density and energy flow characteristics of periodic structures. J Sound Vib 172(4):491–511. https://doi.org/10.1006/jsvi.1994.1191
7. Langley RS, Smith JRD, Fahy FJ (1997) Statistical energy analysis of periodically stiffened damped plate structures. J Sound Vib 208(3):407–426. https://doi.org/10.1006/jsvi.1997.1150
8. Wilson D, Hopkins C (2015) Analysis of bending wave transmission using beam tracing with advanced statistical energy analysis for periodic box-like structures affected by spatial filtering. J Sound Vib 341:138–161. https://doi.org/10.1016/j.jsv.2014.12.029
9. Yan F, Wilson R, Rutherford P, Craik RJM (2016) The use of damping to reduce the contribution of flanking paths to sound transmission in buildings. Noise Control Eng J 64(1):64–74. https://doi.org/10.3397/1/376360
10. Craik RJM (2011) Parallel programmable calculator (PPC). Version 13.320 [computer software] ed. Edinburgh
11. Hopkins C (2002) Statistical energy analysis of coupled plate systems with low modal density and low modal overlap. J Sound Vib 251(2):193–214. https://doi.org/10.1006/jsvi.2001.4002
12. Craik RJM (2001) Contribution of long flanking paths to sound transmission in buildings. Appl Acoust 62(1):29–46. https://doi.org/10.1016/S0003-682X(00)00020-7
13. Yan F, Wilson R, Rutherford P (2020) Prediction of acoustic transmission in heavily damped system using hybrid Ray-Tracing-SEA method. Noise Control Eng J 68(3):226–236. https://doi.org/10.3397/1/376819
14. Yan F, Wilson R, Rutherford P (2020) Numerical study of acoustic transmission across heavily damped plate using hybrid Ray-Tracing-SEA method. Building Acoustics. https://doi.org/10.1177/1351010X20939553
15. Totaro N, Guyader JL (2006) SEA substructuring using cluster analysis: The MIR index. J Sound Vib 290(1–2):264–289. https://doi.org/10.1016/j.jsv.2005.03.030

16. Díaz-Cereceda C, Poblet-Puig J, Rodríguez-Ferran A (2015) Automatic subsystem identification in statistical energy analysis. Mech Syst Signal Process 54–55(mar):182–194
17. Magrans FX, Poblet-Puig J, Rodriguez-Ferran A (2017) A subsystem identification method based on the path concept with coupling strength estimation. Mech Syst Signal Process 100(1):588–604
18. Andrade L, Langley RS, Butlin T, Brett MD, Nielsen OM (2019) Experimental validation of variance estimation in the statistical energy analysis of a structural-acoustic system. ARCHIVE Proc Inst Mech Eng Part C J Mech Eng Sci, 1989–1996 (vols 203–210) 233(18):095440621984357.
19. Poblet-Puig J (2021) Estimation of the coupling loss factors of structural junctions with in-plane waves by means of the inverse statistical energy analysis problem. J Sound Vib 493(3):115850. https://doi.org/10.1016/j.jsv.2020.115850